Journal of Thermal Stresses, 27: 1001–1031, 2004

ISSN: 0149-5739 print/1521-074X online
DOI: 10.1080/01495730490498584

Taylor & Francis
Taylor & Francis Group

CLOSED-FORM SOLUTIONS TO ASSESS MULTILAYERED-PLATE THEORIES FOR VARIOUS THERMAL STRESS PROBLEMS

Erasmo Carrera and Angelo Ciuffreda
Aerospace Department
Politecnico di Torino
Turin, Italy

This paper represents a further development of the first author's works on two-dimensional modeling for thermal stress analysis of multilayered composite plates. The governing equations are written by referring to the unified compact formulation. These equations have been obtained in a form that is not affected by the order of the expansion in the thickness plate direction z or by variable descriptions (layer-wise models and equivalent single layers models). Classical theories based on the principle of virtual displacements and advanced mixed theories based on the Reissner mixed variational theorem are both considered. As a result, a large variety of theories are derived and compared. The temperature profile T_P in the direction z is calculated by solving the heat conduction problem and it is compared to the case in which T_P is assumed linear in z. Exact closed-form solutions have been derived for the case of the in-plane harmonic distribution of displacements, transverse stress variables, and temperature fields. The Fourier expansion was then used to solve problems related to uniform, triangular, bitriangular (tentlike), and localized in-plane distribution of temperature. In some cases more than 25 theories were compared. The effect of transverse shear deformation, the zig-zag form of displacement fields, and interlaminar continuity of transverse stresses (both shear and normal components) have been evaluated in the framework of both classical and mixed theories.

Keywords multilayered plates, composite materials, classical theories, advanced theories, numerical assessment

Temperature variations often represent a contributing factor and sometimes even the predominant cause of failure of engineering structures. These structures often consist of beams, plates, shells, and so forth that are made of multilayered materials. Some examples of multilayered materials can be found in the advanced composite materials that were developed as part of aerospace vehicles (launching/reentry vehicles and fighter aircraft) during the second part of the previous century. Biomedical retinas, reactor vessels, turbines, advanced optical mirrors, semiconductor technologies, and

Received 19 February 2004; accepted 1 June 2004.
Address correspondence to Erasmo Carrera, Aerospace Department, Politecnico di Torino, Corse Duva Degli Abruzzi 24, Turin. 10129, Italy. E-mail: erasmo.carrera@polito.it

space antennas are further examples of multilayered structures that can be subjected to severe thermal environments.

The present work is restricted to flat-plate geometry. As shown in the literature [1–4], exact three-dimensional (3D) solutions have shown that appropriate structural modelings are required to accurately describe multilayered plates. Transverse discontinuous mechanical properties cause displacement fields $\mathbf{u}=(u_x, u_y, u_z)$ (the bold letters denote arrays in an x, y, z Cartesian reference system) in the thickness direction z, which can exhibit a rapid change in slopes corresponding to each layer interface. This is known as the zig-zag (ZZ) effect. However, transverse stresses $\boldsymbol{\sigma}_n = (\sigma_{xz}, \sigma_{yz}, \sigma_{zz})$ must fulfill interlaminar continuity (IC) at each layer interface for equilibrium reasons. Figure 1 shows, from a qualitative point of view, how the distribution of displacements u and transverse stresses $\boldsymbol{\sigma}_n$ could appear whenever exact 3D solutions are provided (or experiments are conducted). Both the displacements and transverse stresses are C^0-continuous functions in the thickness direction z; $\boldsymbol{u}$ and $\boldsymbol{\sigma}_n$ have, in the most general case, discontinuous first derivatives corresponding to each interface where the mechanical properties change. ZZ and IC have been referred to [5] as C_z^0 requirements. The fulfillment of C_z^0 requirements is a crucial point of the two-dimensional modeling of multilayered structures.

Many articles have appeared in which classical and advanced theories have been proposed and applied. Several reviews are available on this topic. Among these, mention can be made of those by Tauchert [6], Noor and Burton [7], Argyris and Tenek [8], as well as that found in the books by Librescu [9], Thornton [10] and Reddy [11]. A discussion of those contributions that are related to the bending of

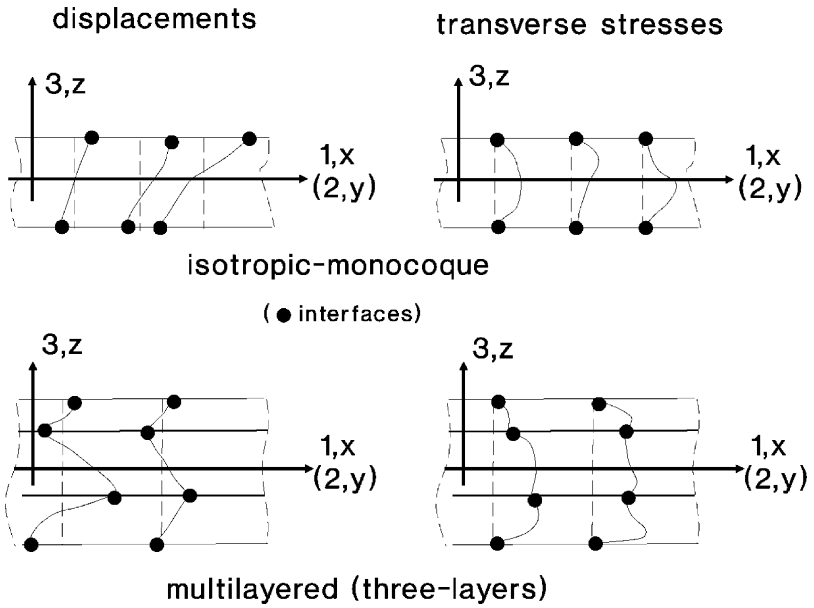

Figure 1. C_z^0 requirements: evidence of ZZ for displacement fields and IC of transverse stresses in the plate thickness direction. Comparison between three-layered and one-layer plates.

anisotropic plates has already been provided [12]. Some recent examples are discussed here. Accurate layerwise theories were developed by Cho, Bert, and Striz [13] and Murakami [14]; a third-order theory was used for each individual layer. According to Reddy [11], these types of theory in which the unknown variables are independent in each layer are known as layerwise models (LWMs). Equivalent single-layer models (ELSMs), in which the unknown variables are the same for the whole plate, were proposed by Ali, Bhaskar, and Varadan [15], who used a cubic displacement field and a Murakami ZZ function for the in-plane displacement components and a parabolic expansion for the transverse displacement. Chattopaday and co-workers [16] developed a third-order theory with a constant and third-order temperature distribution in the thickness direction whose extension to coupled thermopiezoelectric problems was given in by Gu et al. [17].

In most of the available literature, including that concerning 3D solutions (see [4]), the temperature profile $T(z)$ is assumed to be constant or linearly varying across the plate thickness. On the other hand, as discussed by Tungikar and Rao [3], the form of $T(z)$ should be more conveniently taken as a result of solving the heat conduction problem. Interest in a more realistic form of $T(z)$ was displayed in the works by Chattopaday and co-workers [16,17]. Furthermore, it was clearly shown [18] that in spite of the employment of very accurate plate models, inadequate results can occur unless an accurate description of the temperature profiles is made.

Most of the closed-form, analytical solutions given in the previously discussed papers refer to plates loaded by an in-plane harmonic distribution of the temperature fields. In practical problems, the in-plane distribution of temperature can assume different forms: uniform distribution, linear distribution, or localized distribution.

This work is an extension of the recent first author's findings. The aim is twofold. First, the thermomechanical unified formulation of plate theories based on both the principle of virtual displacement (PVD) and the Reissner mixed variational theorem (RMVT) [12, 18] has been extended to assess almost 25 multilayered-plate theories. Second, the closed-form solutions that in [12] and [18] were restricted to the harmonic distribution of the in-plane temperature fields have been extended to include constant, triangular, bitriangular, and localized cases. This has been done by expanding these distributions in terms of Fourier series.

The paper has been organized as follows. The second section compares the two considered cases of temperature profiles, namely the assigned temperature profile and the calculated temperature profile. The third section provides details on the multilayered-plate theories that have been compared in the paper. Classical and advanced mixed theories formulated in both the ESLM and LWM framework are discussed. Well-known plate theories such as classical lamination theory (CLT) and first-order shear deformation theory (FSDT) are included in the comparison. Displacement and transverse stress models of the various theories have been written in a unified form. This unified form was used in the fourth section to derive the governing equations of each layer for PVD and RMVT applications. Extensive use of subscripts and superscripts has been made. Multilayered equations are outlined by introducing the C_z^0 requirements. The numerical analyses have been documented in the fifth section.

TEMPERATURE PROFILE ACROSS THE PLATE THICKNESS

A laminated plate, made of N_l orthotropic layers, has been considered (see Figure 2). In this context, x, y, z is a system of Cartesian coordinates and a, b, and h are the plate dimensions with respect to the defined coordinates. The principal material directions of the constitutive layers coincide with the geometric axes. As done by Tungikar and Rao [3], attention was here restricted to the particular case in which the multilayered plate is subjected to the following conditions on the upper and bottom faces:

$$\begin{aligned} T &= 0 && \text{at } x = 0 \quad \text{and} \quad y = 0, b \\ T &= T_b \sin\frac{m\pi}{a}x \sin\frac{m\pi}{b}y && \text{at } z = -\frac{h}{2} \\ T &= T_t \sin\frac{m\pi}{a}x \sin\frac{m\pi}{b}y && \text{at } z = \frac{h}{2} \end{aligned} \tag{1}$$

where m and n are the wave numbers along the plate width and length, a and b, respectively.

The continuity conditions for the temperature and heat flux q_z in the thickness direction, at each k-layer interface, are

$$\begin{aligned} T^k &= T^{k+1} \\ q^k &= T^{k+1} \qquad k = 1, N_l - 1 \end{aligned} \tag{2}$$

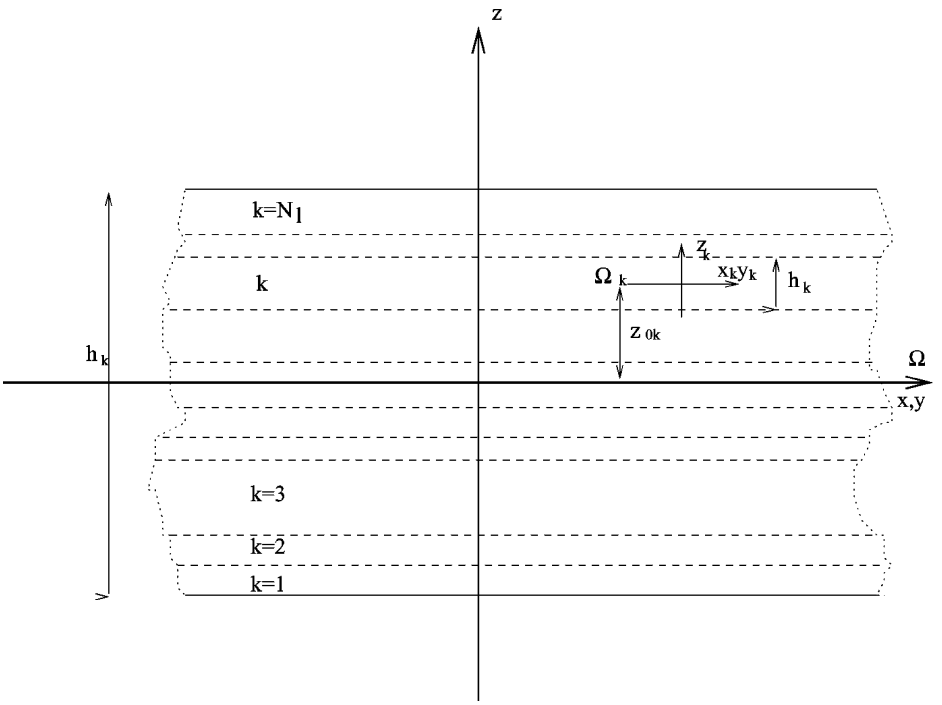

Figure 2. Plate geometry and notations.

where the relationship between the heat flux and the temperature is as follows:

$$q_z^k = K_3^k \frac{\partial T^k}{\partial z} \tag{3}$$

while $K_3 = K_z$ represents the thermal conductivity of the k layer in the z direction. For a homogeneous orthotropic material the differential Fourier equation of heat conduction is

$$K_1 \frac{\partial^2 T}{\partial x^2} + K_2 \frac{\partial^2 T}{\partial y^2} + K_3 \frac{\partial^2 T}{\partial z^2} = 0 \tag{4}$$

where K_1 and K_2 are the thermal conductivities in the in-plane x and y directions, respectively.

The preceding set of governing equations can be solved in the spirit of the method described in the literature [3, 18]. The following temperature profile is found for the kth layer:

$$T_c(z) = T^k = (C_1^k \cosh s_1 z + C_2^k \sinh s_1 z) \sin \frac{m\pi}{a} x \sin \frac{m\pi}{b} y \tag{5}$$

The $2 \times N_l$ constants C_1^k, C_2^k are determined by imposing the previously specified continuity conditions for the heat flux q_z and the temperature at $N_l - 1$ interfaces, [e.g., Eq. (2)] along with the two additional conditions at the top−bottom surface for T.

To preserve consistency with the employed plate theories (see next sections) and without losing generality, the calculated temperature $T_a(z)$ given by Eqs. (5) has been expressed by using the same base function employed for transverse stress and displacement variables (see third section):

$$T^k(x, y, z) = F_t \, T_t^k \; + \; F_b \, T_b^k \; + \; F_2 \, T_2^k = F_\tau \, T_\tau^k \tag{6}$$

where F_τ is a combination of Legendre (or power of z) polynomials. More details related to this equation will be provided later.

A comparison between a linear and calculated temperature profile for a three-layered plate is shown in Figure 3. The data for this problem are given in "Fourier Analyses of Various Temperature Distributions." The top (T_t) and bottom (T_b) plate temperatures refer to an environmental temperature T_e. The following data are considered:

$$\frac{T_t}{T_e} = 1 \qquad \frac{T_b}{T_e} = -1$$

The calculated temperature profile in Eq. 5 is compared to the assigned linear one:

$$\frac{T_a(z)}{T_e} = \frac{T_0}{T_e} \frac{2z}{h}$$

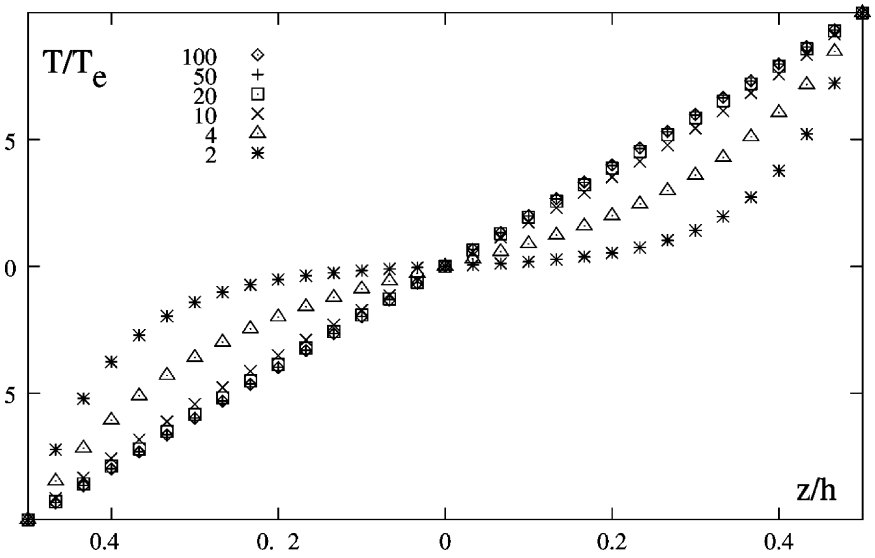

Figure 3. Calculated temperature profile T_c for various plate/thickness parameters.

Various thickness parameters were considered. The obtained results show that

- the temperature distribution approaches the linear case if, and only if, the thin-plate cases are considered;
- the calculated temperature profiles for thick plates feature an intrinsic layerwise description.

THEORIES COMPARED IN THIS WORK

Classical Lamination Theory

The simplest known plate theory, namely CLT, is based on Kirchhoff thin-plate assumptions (see [11]). Transverse shear strains as well as transverse normal strains are neglected. In the framework of CLT applications, the displacement is represented by

$$\begin{aligned} u_i &= u_i^0 - z\, u_{z,i} \qquad i = x, y \\ u_z &= u_z^0 \end{aligned} \tag{7}$$

where superscript 0 denotes displacement values on Ω, which is the reference plane of the plate (usually the midsurface of the plate). The comma denotes partial derivatives.

First-Order Shear Deformation Theory

The inclusion of transverse shear strains leads to the following representation of the displacement quantities:

$$\begin{aligned} u_i &= u_i^0 + z\,\phi_i \qquad i = x, y \\ u_z &= u_z^0 \end{aligned} \tag{8}$$

This FSDT is also known as the Reissner–Mindlin plate theory (see [11]). In this theory a first-order Taylor-type expansion of displacement unknowns in the neighborhood of the reference surface Ω is considered; ϕ_x, ϕ_y represents the rotations of the normal to Ω in the two planes x–z and y–z, respectively. These rotations can also be expressed in terms of transverse shear strains:

$$\phi_x = \epsilon_{xz} - u_{3,x} \qquad \phi_y = \epsilon_{yz} - u_{3,y}$$

The FSDT model can be rewritten according to the following array form:

$$\boldsymbol{u}(x, y, z) = F_0(z)\,\boldsymbol{u}_0(x, y) \;+\; F_1(z)\,\boldsymbol{u}_1(x, y) \tag{9}$$

The polynomials used in the expansion take on the following values:

$$F_0(z) = 1 \qquad F_1(z) = z$$

The bold lettering denotes arrays:

$$\boldsymbol{u}_0(x, y) = (u_{x_0}(x, y), u_{y_0}(x, y), u_{z_0}(x, y)) \qquad \boldsymbol{u}_1(x, y) = (u_{x_1}(x, y), u_{y_1}(x, y), u_{z_1}(x, y))$$

The displacement unknowns are

$$u_{x_0}(x, y) = u_x^0 \qquad u_{y_0} = u_y^0 \qquad u_{z_0}(x, y) = u_z^0 \qquad u_{x_1}(x, y) = \phi_x \qquad u_{y_1} = \phi_y$$

and

$$u_{z_1}(x, y) = 0 \tag{10}$$

This last condition underlines that transverse normal strains are discarded in FSDT formulated plate modelings.

Incorporation of Transverse Normal Strains in the FSDT: ED1 Theory

Transverse normal strains can be included by generalizing the representation provided in Eq. (8) and incorporating the transverse normal strain. The explicit form of the displacement field is

$$\begin{aligned} u_x &= F_0(z)\,u_{0_x} + F_1(z)\,u_{1_x} \\ u_y &= F_0(z)\,u_{0_y} + F_1(z)\,u_{1_y} \\ u_z &= F_0(z)\,u_{0_z} + F_1(z)\,u_{1_z} \end{aligned} \tag{11}$$

The related plate theory is hereafter referred to with the acronym ED1: this is an ESLM with only displacement unknowns and a Taylor expansion truncated at the first order $N = 1$.

An FSDT model can be considered a particular case of ED1 in which the constraints expressed by Eq. (10) are imposed. CLT results were obtained in this work from FSDT analyses by applying a penalty technique to the shear correction factor.

Higher Order Theories: EDN

The ED1 displacement model can be easily extended to a higher order Taylor expansion. Such an expansion can be herein written in array form:

$$\begin{aligned}\boldsymbol{u}(x,y,z) = {} & F_0(z)\,\boldsymbol{u}_0(x,y) \\ & + F_1(z)\,\boldsymbol{u}_1(x,y) + \cdots + \cdots + F_N(z)\,\boldsymbol{u}_N(x,y)\end{aligned} \tag{12}$$

or, by introducing Einstein's convention for repeated indices,

$$\boldsymbol{u}(x,y,z) = F_\tau(z)\,\boldsymbol{u}_\tau(x,y) \qquad \tau = 0, N \tag{13}$$

where

$$F_\tau(z) = z^\tau$$

For the sake of convenience, this displacement model is put in the form

$$\boldsymbol{u}(x,y,z) = F_t(z)\boldsymbol{u}_t(x,y) + F_b(z)\boldsymbol{u}_b(x,y) + F_\tau(z)\boldsymbol{u}_\tau(x,y) \qquad \tau = 2, N \tag{14}$$

where

$$F_t(z) = 1 \qquad F_b(z) = z \qquad F_\tau(z) = z^\tau \qquad \tau = 2, N$$

With respect to Eqs. (12), the constant and linear terms are now denoted with subscript t and b, respectively.

Incorporation of Zig-Zag Effects via the Murakami ZZ Function: EDZ

The EDN models are not able to describe the ZZ effect. The discontinuity of the first derivative at the layer interfaces, in the ESLM framework, can be incorporated by employing the Murakami ZZ function (MZZF) that was originally proposed [19] in the framework of RMVT applications.

According to Figure 2, z is the thickness coordinate of the whole multilayer while z_k is the layer thickness coordinate. The dimensionless layer coordinate $\zeta_k = z_k/2h_k$ (h_k is the thickness of the kth layer) is considered. The MZZF $M(z)$ was defined according to the following formula [19]:

$$M(z) = (-1)^k \zeta_k \tag{15}$$

$M(z)$ has the following properties. It is a piecewise linear function of the layer coordinates z_k; $M(z)$ has unit amplitude for the whole layers; and the slope $M'(z) = dM/dz$ assumes opposite signs between two adjacent layers (its amplitude is layer thickness dependent). A plot of $M(z)$ is given in Figure 4. The displacement that includes MZZF is written in the form

$$\boldsymbol{u} = \boldsymbol{u}_0 + (-1)^k \zeta_k \mathbf{u}_Z + z^r \mathbf{u}_r \qquad r = 1, 2, \ldots, N \tag{16}$$

The subscript Z refers to the introduced ZZ term. Higher order distributions in the z direction are introduced by the r polynomials. The displacement model is therefore

ZZ effects can be more conveniently imposed by employing interface values as unknown variables:

$$\boldsymbol{u}^k_{nM} = F_t \boldsymbol{u}^k_{nt} + F_b \boldsymbol{u}^k_{nb} + F_r \boldsymbol{u}^k_{nr} = F_\tau \boldsymbol{u}^k_{n\tau} \qquad \tau = t,b,r \qquad r = 2,3,\ldots,N \qquad k = 1,2,\ldots,N_l \tag{18}$$

In contrast to Eqs. (17), subscripts t and b denote values related to the layer top and bottom surfaces, respectively. They consist of the linear part of the expansion. The thickness functions $F_\tau(\zeta_k)$ have been defined by

$$F_t = \frac{P_0 + P_1}{2} \qquad F_b = \frac{P_0 - P_1}{2} \qquad F_r = P_r - P_{r-2} \qquad r = 2,3,\ldots,N \tag{19}$$

in which $P_j = P_j(\zeta_k)$ is the Legendre polynomial of the jth order defined in the ζ_k domain $-1 \leq \zeta_k \leq 1$. From linear up to fourth-order expansions will be used in the numerical investigations; the related polynomials are

$$P_0 = 1 \qquad P_1 = \zeta_k \qquad P_2 = (3\zeta_k^2 - 1)/2$$
$$P_3 = \frac{5\zeta_k^3}{2} - \frac{3\zeta_k}{2} \qquad P_4 = \frac{35\zeta_k^4}{8} - \frac{15\zeta_k^2}{4} + \frac{3}{8}$$

The chosen functions have the following properties:

$$\zeta_k = \begin{cases} 1 : F_t = 1; F_b = 0; F_r = 0 \\ -1 : F_t = 0; F_b = 1; F_r = 0 \end{cases} \tag{20}$$

The top and bottom values have been used as unknown variables. The interlaminar compatibility of displacement can therefore be easily linked:

$$\boldsymbol{u}^k_t = \boldsymbol{u}^{(k+1)}_b \qquad k = 1, N_l - 1 \tag{21}$$

Fulfillment of IC via RMVT Applications

A possible way of addressing the complete and a priori fulfillment of ZZ and IC is to refer to RMVT applications [20, 21, 22]. According to RMVT statements, displacements $\boldsymbol{u}$ and transverse stresses $\boldsymbol{\sigma}_n = (\sigma_{xz}, \sigma_{yz}, \sigma_{zz})$ can be independently assumed. Formally, both the previously discussed Taylor and Legendre expansions can be used. In practice (see [21]), transverse stress demands a Legendre layerwise expansion, whereas both expansions can be used for the displacements. In a unified form the displacement and stress fields are expressed as

$$\begin{aligned} \boldsymbol{u}^k &= F_t \boldsymbol{u}^k_t + F_b \boldsymbol{u}^k_b + F_r \boldsymbol{u}^k_r = F_\tau \boldsymbol{u}^k_\tau \qquad && \tau = t,b,r \\ & && r = 2,3,\ldots,N \\ \boldsymbol{\sigma}^k_{nM} &= F_t \boldsymbol{\sigma}^k_{nt} + F_b \boldsymbol{\sigma}^k_{nb} + F_r \boldsymbol{\sigma}^k_{nr} = F_\tau \boldsymbol{\sigma}^k_{n\tau} \qquad && k = 1,2,\ldots,N_l \end{aligned} \tag{22}$$

The top and bottom values have also been used as unknown variables. The interlaminar transverse shear and normal stress continuity can therefore be easily linked:

$$\boldsymbol{\sigma}_{nt}^{k} = \boldsymbol{\sigma}_{nb}^{(k+1)} \qquad k = 1, N_l - 1 \tag{23}$$

In those cases in which top/bottom-plate stress values are prescribed (zero or imposed values), the following additional equilibrium conditions must be accounted for:

$$\boldsymbol{\sigma}_{nb}^{1} = \bar{\boldsymbol{\sigma}}_{nb} \qquad \boldsymbol{\sigma}_{nt}^{N_l} = \bar{\boldsymbol{\sigma}}_{nt} \tag{24}$$

where the overbar denotes the imposed values corresponding to the plate boundary surfaces (which have been assumed zero in what follows).

The MZZF must be used to describe ZZ effects in the case of an ESLM description.

Summary of the Acronyms Used in this Work

Depending on the type of formulation (PVD or RMVT), the variables description (LWM or ESLM), the order of the expansion used, and so on, a number of two-dimensional theories can be generated on the basis of the two-dimensional modelings described in this section. To identify these theories pertinent acronyms will be extensively used. Figure 6 shows how such acronyms have been built. Examples of

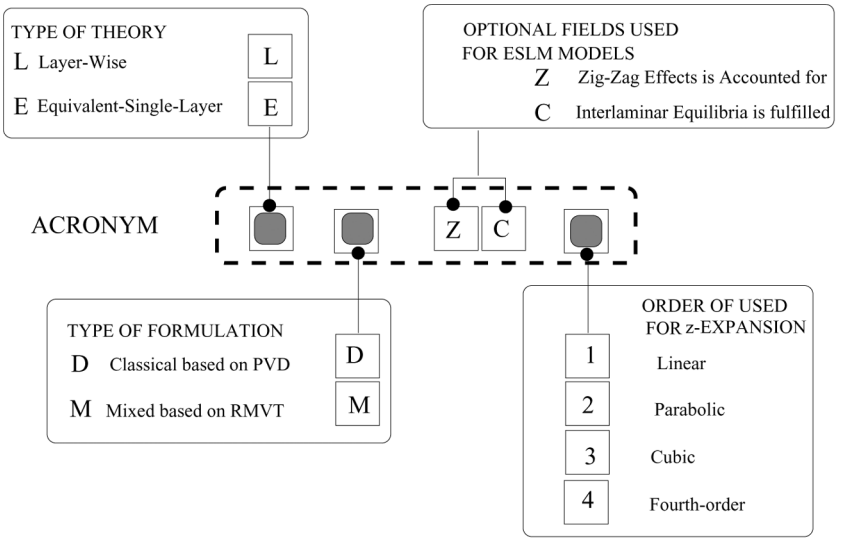

Figure 6. Acronyms that have been used to denote the various theories.

displacement and stress fields related to a few particular case theories are discussed in the following. The transverse stress and displacement z fields are the same for layerwise mixed linear (LM1) and layerwise mixed cubic (LM3) descriptions whereas only displacement assumptions are considered for layerwise displacement linear (LD1) and layerwise displacement cubic (LD3) cases. The parabolic transverse stress field in each layer is associated with a linear ZZ displacement field for the equivalent-single-layer mixed Zig-Zag interlaminar-Continuity linear (EMZC1) case and a fourth-order transverse stress field in each layer is associated with the cubic ZZ displacement field for the equivalent-single-layer mixed zig-zag interlaminar-continuity cubic (EMZC3) case.

UNIFIED FORMS OF GOVERNING EQUATIONS

The differential equations and boundary conditions governing the thermomechanical response of a layered plate for the theories described in the previous paragraph have already been derived in the first author's paper [12], where more details are provided. Herein a few hints are provided for the sake of completeness.

Classical Theories Based on PVD

For the thermoelastic case the classical displacement approach is formulated in terms of $\boldsymbol{u}^k$ via the principle of virtual displacements as

$$\sum_{k=1}^{N_l} \int_{\Omega^k} \int_{A_k} (\delta \boldsymbol{\epsilon}_{pG}^{kT} (\boldsymbol{\sigma}_{pH_d}^k - \boldsymbol{\sigma}_{pT}^k) + \delta \boldsymbol{\epsilon}_{nG}^{kT} (\boldsymbol{\sigma}_{nH_d}^k - \boldsymbol{\sigma}_{nT}^k))\, d\Omega^k dz = \delta L^e \tag{25}$$

where δ is the variational symbol and the subscript T denotes the transposition of arrays; A_k and V denote the layer-thickness domain and the volume, respectively; Ω^k is the middle surface of the layer which is bounded by Γ^k. (Γ_g^k, Γ_m^k denotes those parts of Γ^k on which the geometrical and mechanical boundary conditions are prescribed.) The variation of the internal work has been split into the in-plane and out-of-plane parts and involves stress from Hooke's law and strain from geometrical relations. δL_e is the virtual variation of the work made by the external layer forces $\boldsymbol{p}^k = \{p_x^k, p_y^k, p_z^k\}$.

Based on the previous stated assumptions, Eq. (25) leads to the following equilibrium equations on Ω^k for each k layer:

$$\delta \boldsymbol{u}_\tau^k : -\boldsymbol{D}_p^T (\mathcal{R}_{pH_d}^{k\tau} - \mathcal{R}_{pT}^{k\tau}) + \mathcal{R}_{nH_d}^{k\tau_z} + \mathcal{R}_{nT}^{k\tau_z} - D_{n\Omega}^T (\mathcal{R}_{nH_d}^{k\tau} - \mathcal{R}_{nT}^{k\tau}) = \boldsymbol{p}_\tau^k \tag{26}$$

while the boundary conditions on Γ^k are, geometric on Γ_g^k,

$$\boldsymbol{u}_\tau^k = \bar{\boldsymbol{u}}_\tau^k$$

or static on Γ_m^k

$$\mathbf{I}_p^T (\mathcal{R}_{pH_d}^{k\tau} - \mathcal{R}_{pT}^{k\tau}) + \mathbf{I}_{n\Omega}^T (\mathcal{R}_{nH_d}^{k\tau} - \mathcal{R}_{nT}^{k\tau}) = \mathbf{I}_p^T (\bar{\mathcal{R}}_{pH_d}^{k\tau} - \bar{\mathcal{R}}_{pT}^{k\tau}) + \mathbf{I}_{n\Omega}^T (\bar{\mathcal{R}}_{nH_d}^{k\tau} - \bar{\mathcal{R}}_{nT}^{k\tau}) \tag{27}$$

The following stress layer resultants are defined:

$$(\mathcal{R}^{k\tau}_{pH_d}, \mathcal{R}^{k\tau}_{nH_d}, \mathcal{R}^{k\tau z}_{nH_d}) = \int_{A_k} (F_\tau \boldsymbol{\sigma}^k_{pH_d}, F_\tau \boldsymbol{\sigma}^k_{nH_d}, F_{\tau z} \boldsymbol{\sigma}^k_{nH_d})\, dz$$
$$(\mathcal{R}^{k\tau}_{pT}, \mathcal{R}^{k\tau}_{nT}, \mathcal{R}^{k\tau_z}_{nT}) = \int_{Ak} (F_\tau \boldsymbol{\sigma}^k_{pT}, F_\tau \boldsymbol{\sigma}^k_{nT}, F_{\tau_z} \boldsymbol{\sigma}^k_{nT})\, dz \tag{28}$$

The bar denotes imposed values at the boundary. The complete set of equations for the N_l layers can be written simply by expanding the considered subscripts and superscripts over their ranges (see [12]).

The obtained form of the governing equations is the same for all theories based on PVD. These can be written in terms of the unknown displacements according to the statements detailed in the literature [21].

Advanced Mixed Theories Based on RMVT

In the case of mixed-plate theories, equilibrium and compatibility are both formulated in terms of the $\boldsymbol{u}^k$ and $\boldsymbol{\sigma}^k_n$ unknowns via Reissner's variational equation [20, 21]:

$$\sum_{k=1}^{N_l} \int_{\Omega^k} \int_{A_k} (\delta \boldsymbol{\epsilon}^{k\,T}_{p\,G} (\boldsymbol{\sigma}^k_{p\,H} - \boldsymbol{\sigma}^k_{p\,T}) + \delta \boldsymbol{\epsilon}^{k\,T}_{n\,G} \boldsymbol{\sigma}^k_{n\,M} + \delta \boldsymbol{\sigma}^{k\,T}_{n\,M} (\boldsymbol{\epsilon}^k_{n\,G} - (\boldsymbol{\epsilon}^k_{n\,H} - \boldsymbol{\epsilon}^k_{n\,T})))\, d\Omega^k dz = \delta L^e \tag{29}$$

The left-hand side includes the variations of the internal work in the plate: the first two terms come from the displacement formulation and lead to variationally consistent equilibrium conditions; the third "mixed" term variationally enforces the compatibility of the transverse strain components.

By imposing the definition of virtual variations for the unknown stress and displacement variables, the differential system of the governing equations and related boundary conditions for the kth layer are obtained in terms of the introduced stress and strain resultants.

The equilibrium equations on Ω^k are

$$\delta \boldsymbol{u}^k_\tau : -\mathbf{D}^T_p (\mathcal{R}^{k\tau}_{pH} - \mathcal{R}^{k\tau}_{pT}) + \mathcal{R}^{k\tau_z}_{nM} - \mathbf{D}^T_{n\Omega} \mathcal{R}^{k\tau}_{nM} = \boldsymbol{p}^k_\tau \tag{30}$$

The constitutive equations on Ω^k are, geometric

$$\delta \boldsymbol{\sigma}^k_{n\tau} : \mathcal{S}^{k\tau}_{nG} - (\mathcal{S}^{k\tau}_{nH} - \mathcal{S}^{k\tau}_{nT}) = 0 \tag{31}$$

The boundary conditions on Γ^k are, geometric on Γ^k_g,

$$\boldsymbol{u}^k_\tau = \bar{\boldsymbol{u}}^k_\tau \tag{32a}$$

or static on Γ^k_m

$$\mathbf{I}^T_p \mathcal{R}^{k\tau}_{pH} + \mathbf{I}^T_{n\Omega} \mathcal{R}^{k\tau}_{nM} = \mathbf{I}^T_p \bar{\mathcal{R}}^{k\tau}_{pH} + \mathbf{I}^T_{n\Omega} \bar{\mathcal{R}}^{k\tau}_{nM} \tag{32b}$$

The additional stress and strain layer resultants have been defined:

$$(\mathcal{R}^{k\tau}_{pH}, \mathcal{R}^{k\tau}_{nM}, \mathcal{R}^{kt_z}_{nM}, \mathcal{S}^{k\tau}_{nG}, \mathcal{S}^{k\tau}_{nH}, \mathcal{S}^{k\tau}_{nT}) = \int_{A_k} (F_\tau \boldsymbol{\sigma}^k_{pH}, F_\tau \boldsymbol{\sigma}^k_M, F_{\tau_z} \boldsymbol{\sigma}^k_M, F_\tau \epsilon^k_{nG}, F_\tau \epsilon^k_{nH}, F_\tau \epsilon^k_{nT})\, dz \tag{33}$$

The obtained form of the governing equations is the same for the all the theories based on RMVT applications. These can be written in terms of the unknown displacements and stresses according to the statements detailed in the literature [21].

Governing Equations for the Multilayered Plate

The previous subsections have presented the governing equations of PVD and RMVT cases for the N_l single layers. The continuity conditions of displacement and transverse stress variables (the C^0_z requirements) can be accounted for by simply writing the governing equations at the multilayered level (see Figure 7). First the equations must be written in terms of unknown displacement and transverse stress variables. The necessary steps have been extensively explained in the first author's previous works [5, 21]. By choosing the top and r variables as layer unknowns, the arrays of the unknown displacements for the whole multilayer hold:

$$\boldsymbol{u}^T = \left\{ \boldsymbol{u}^{1^T}_b, \boldsymbol{u}^{1^T}_t, \boldsymbol{u}^{1^T}_2; \boldsymbol{u}^{2^T}_t, \boldsymbol{u}^{2^T}_2; \ldots \boldsymbol{u}^{k^T}_t, \boldsymbol{u}^{k^T}_2; \right.$$
$$\left. \boldsymbol{u}^{(k+1)^T}_t, \boldsymbol{u}^{(k+1)^T}_2; \ldots; \boldsymbol{u}^{(N_l-1)^T}_t, \boldsymbol{u}^{(N_l-1)^T}_2; \boldsymbol{u}^{N_l{}^T}_t, \boldsymbol{u}^{N_l{}^T}_2 \right\} \tag{34}$$

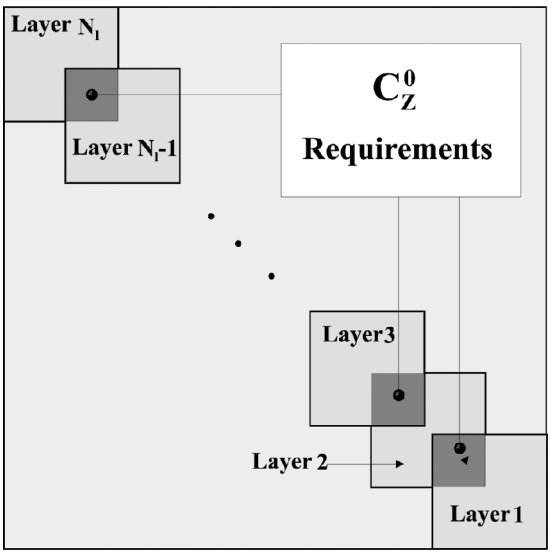

Figure 7. An example showing how the C^0_z requirements are imposed from layer to multilayer level.

The governing equations for the displacement formulation are formally written as

$$\begin{aligned} &\boldsymbol{K}_d\,\boldsymbol{u} = \boldsymbol{p} \\ &\boldsymbol{u} = \bar{\boldsymbol{u}} \quad \text{or } \Pi_d \boldsymbol{u} = \Pi_d \bar{\boldsymbol{u}} \end{aligned} \tag{35}$$

where the vector $\boldsymbol{p}$ includes the thermal and mechanical loadings. By defining a stress array for the entire multilayer,

$$\boldsymbol{\sigma}_n{}^T = \left\{ \boldsymbol{\sigma}_{nt}^{1T}, \boldsymbol{\sigma}_{n2}^{1T}; \boldsymbol{\sigma}_{nt}^{2T}, \boldsymbol{\sigma}_{n2}^{2T}; \ldots \boldsymbol{\sigma}_{nt}^{kT}, \boldsymbol{\sigma}_{n2}^{kT}; \boldsymbol{\sigma}_{nt}^{(k+1)^T}, \boldsymbol{\sigma}_{n2}^{(k+1)^T}; \ldots; \boldsymbol{\sigma}_{nt}^{(N_l-1)^T}, \boldsymbol{\sigma}_{n2}^{(N_l-1)^T}; \boldsymbol{\sigma}_{n2}^{N_l T} \right\} \tag{36}$$

the governing system of differential equations at the multilayer level for the mixed cases is formally written in the following final form:

$$\begin{aligned} &\boldsymbol{K}_{uu}\,\boldsymbol{u} + \boldsymbol{K}_{u\boldsymbol{\sigma}}\,\boldsymbol{\sigma}_n = \boldsymbol{p} \\ &\boldsymbol{K}_{\sigma u}\boldsymbol{u} + \boldsymbol{K}_{\sigma\sigma}\,\boldsymbol{\sigma}_n = 0 \end{aligned} \tag{37}$$

The boundary conditions are

$$\boldsymbol{u} = \bar{\boldsymbol{u}} \text{ or } \Pi_u \boldsymbol{u} + \Pi_\sigma \boldsymbol{\sigma}_n = \Pi_u \bar{\boldsymbol{u}} + \Pi_\sigma \bar{\boldsymbol{\sigma}}_n + \mathbf{q}_\sigma^{1N_l} \tag{38}$$

For the sake of brevity, the explicit form of the multilayer governing equations has been omitted. Figures 8 and 9 show how the stiffness/compliance of different layers takes place in the multilayered arrays. (This is, in fact, the assemblage process from the N_l single layers to the multilayered plates.) The ESLM and LWM cases have both been considered in these two figures.

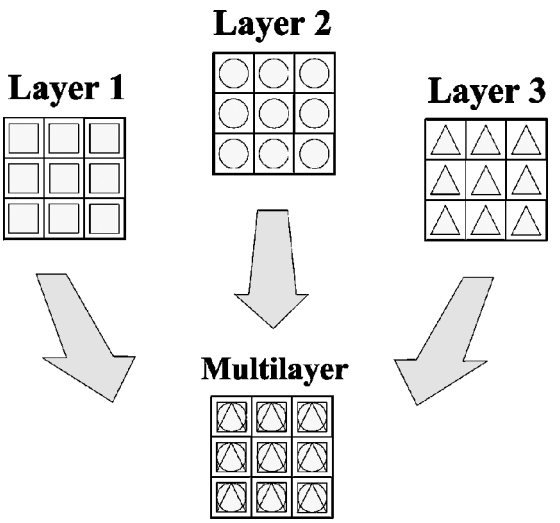

Figure 8. Assemblage from layer to multilayered level in ESLM case for a three-layered plate.

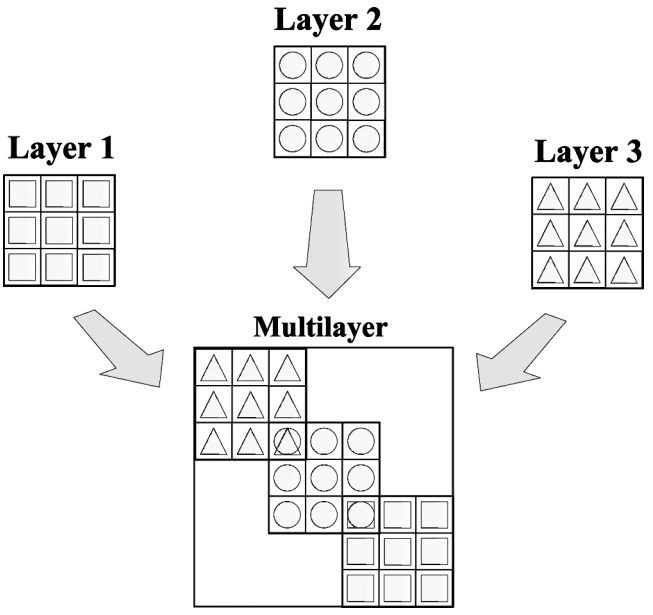

Figure 9. Assemblage from layer to multilayered level in LWM case for a three-layered plate.

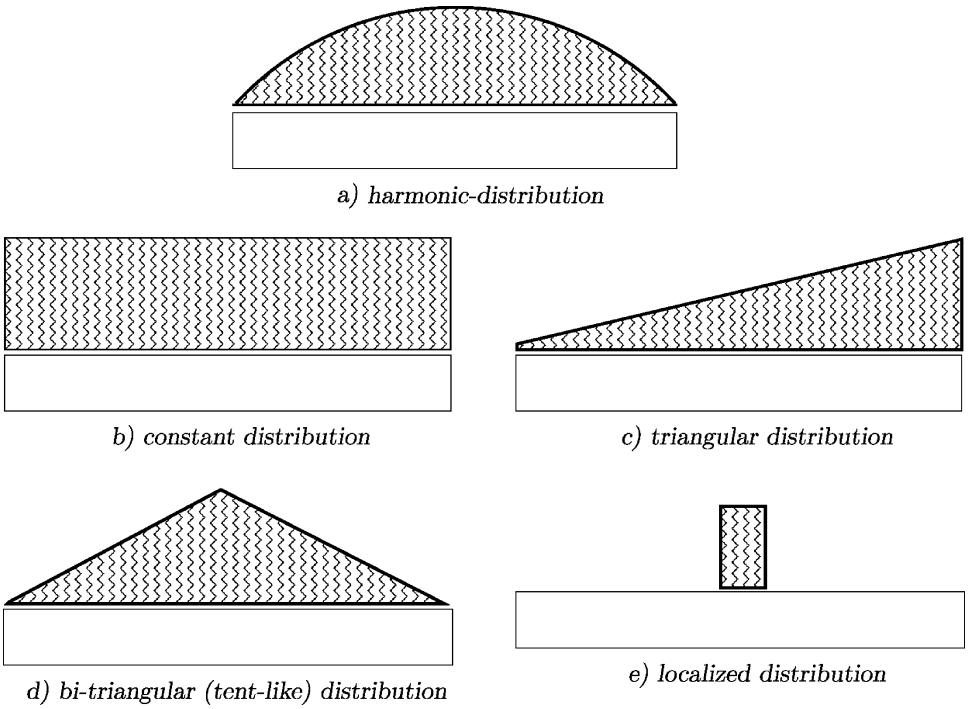

Figure 10. Various in-plane temperature distributions for which closed-form solutions have been provided in the present work.

Table 1 Transverse displacement and transverse shear stress of thick and thin plates. Comparison of different theories to exact solutions

	$\bar{U}_z$ at $z = \mp h/2$		S_{xz} at $z = \mp h/6$	
	4	100	4	100
a/h				
Exact	42.69	10.26	84.81	7.073
Layerwise Theories				
	RMVT Applications			
LM4	42.69	10.26	84.81	7.073
LM3	42.70	10.26	84.85	7.073
LM2	42.74	10.26	84.90	7.073
LM1	42.62	10.33	94.74	7.498
	PVD Applications, no IC			
LD4	42.69	10.26	84.81	7.073
LD3	42.68	10.26	84.82	7.073
LD2	42.25	10.26	82.92	7.073
LD1	41.24	10.92	235.4	7.672
Equivalent Single Layer Theories				
	RMVT Applications			
			Including ZZ and IC	
EMZC3	42.44	10.26	83.81	7.073
EMZC2	41.99	10.26	89.04	7.074
EMZC1	36.96	16.12	116.3	9.198
			Including IC	
EMC4	42.18	10.25	96.37	7.076
EMC3	42.26	10.25	96.15	7.076
EMC2	34.76	10.23	120.16	7.079
EMC1	30.64	16.09	150.39	9.205
	PVD Applications			
			Including ZZ	
EDZ3	42.34	10.26	96.4	7.076
EDZ2	17.00	10.26	102.72	7.077
EDZ1	36.61	16.12	137.04	9.203
			Discarding IC and ZZ	
ED4	42.05	10.25	88.64	7.075
ED3	42.04	10.25	88.62	7.075
ED2	34.74	10.23	116.2	7.079
ED1	30.42	16.09	144.2	9.204
FSDT	30.42	16.09	151.8	9.206
CLT	10.18	10.18	177.1	7.089

CLOSED-FORM SOLUTIONS FOR THE HARMONIC DISTRIBUTION OF TEMPERATURE

Exact, closed-form solutions of the derived system of differential equations that govern the thermomechanical response of a generally laminated multilayered plate are not available. Approximate solution procedures could conveniently be implemented for this purpose [5]. The particular case in which the material has the following

Table 2 Influence of thickness ratio to transverse displacement $\bar{U}_z$. Comparison between assigned and calculated temperature profiles for advanced mixed theories formulated on the basis of RMVT

		a/h			
Theory	$T(z)$	2	4	10	100
RMVT Applications					
3D	T_a	96.79	42.69	17.39	10.26
	T_c	—	—	—	—
			Layerwise Theories (no IC)		
LM4	T_a	96.79	42.69	17.39	10.26
	T_c	75.60	37.91	16.92	10.26
LM3	T_a	96.77	42.68	17.39	10.26
	T_c	104.77	43.06	15.86	8.53
LM2	T_a	95.74	42.55	17.39	10.26
	T_c	109.43	56.29	25.15	14.64
LM1	T_a	96.86	42.62	17.36	10.33
	T_c	81.31	38.90	16.96	10.33
			Equivalent Single-Layer Theories Including ZZ and IC		
EMZC3	T_a	95.26	42.42	17.38	10.26
	T_c	40.83	30.52	15.53	10.24
EMZC2	T_a	93.74	41.44	17.04	10.26
	T_c	3.79	15.74	18.55	16.09
EMZC1	T_a	50.82	36.65	21.63	16.16
	T_c	37.88	15.74	18.55	16.09
			Theories including IC		
EMC4	T_a	98.26	42.18	16.96	10.25
	T_c	40.70	30.34	15.17	10.24
EMC3	T_a	98.16	42.26	17.00	10.25
	T_c	25.82	29.50	16.01	10.25
EMC2	T_a	83.12	34.76	14.98	10.23
	T_c	6.19	14.93	12.85	10.22
EMC1	T_a	42.29	30.64	19.61	16.09
	T_c	3.15	13.16	16.81	16.08

properties, $\tilde{C}_{16} = \tilde{C}_{26} = \tilde{C}_{36} = \tilde{C}_{45} = 0$, has been considered here. In such a case, Navier-type closed-form solutions can be found by assuming the following harmonic forms for the applied mechanical and thermal loadings and unknown variables:

$$
\begin{aligned}
(u^k_{x_r}, \sigma^k_{xz_r}, p^k_{x_r}) &= \sum\nolimits_{m,n} (U^k_{x_r}, S^k_{xz_r}, P^k_{x_r}) \cos\frac{m\pi x}{a} \sin\frac{n\pi y}{b} \\
(u^k_{y_r}, \sigma^k_{yz_r}, p^k_{y_r}) &= \sum\nolimits_{m,n} (U^k_{y_r}, S^k_{yz_r}, P^k_{y_r}) \sin\frac{m\pi x}{a} \cos\frac{n\pi y}{b} \\
(u^k_{z_r}, \sigma^k_{zz_r}, p^k_{z_r}) &= \sum\nolimits_{m,n} (U^k_{z_r}, S^k_{zz_r}, P^k_{z_r}) \sin\frac{m\pi x}{a} \sin\frac{n\pi y}{b} \\
T(x,y,z) &= T_P(z) \sin\frac{m\pi x}{a} \sin\frac{n\pi y}{b}
\end{aligned}
\tag{39}
$$

which correspond to simply supported boundary conditions. Here, m and n are wave numbers in the x and y directions, respectively, while a and b are the plate width and length, respectively. The capital letters on the right-hand side denote the corresponding maximum amplitudes. Upon substitution of Eqs. (39) the governing equations written in the previous subsections assume the form of a linear system of algebraic equations whose solutions are discussed in the next section.

Table 3 Influence of thickness ratio to transverse displacement $\bar{U}_z$. Comparison between assigned and calculated temperature profiles for classical theories formulated on the basis of PVD

		a/h			
Theory	$T(z)$	2	4	10	100
3D	T_a	96.79	42.69	17.39	10.26
	T_c	—	—	—	—
PVD Applications					
			Layerswise Theories		
LD4	T_a	96.78	42.69	17.39	10.26
	T_c	75.16	37.91	16.92	10.26
LD3	T_a	96.73	42.68	17.39	10.26
	T_c	104.76	43.06	15.86	8.53
LD2	T_a	94.34	42.25	17.36	10.26
	T_c	108.37	55.88	25.09	14.64
LD1	T_a	89.25	41.24	17.92	10.91
	T_c	73.73	37.30	17.19	10.91
			Equivalent Single-Layer Theories		
			Including ZZ		
EDZ3	T_a	94.87	42.34	17.37	10.26
	T_c	40.82	30.49	15.52	10.24
EDZ2	T_a	93.26	41.34	17.00	10.26
	T_c	6.95	17.76	14.58	10.24
EDZ1	T_a	50.06	36.61	21.61	16.12
	T_c	3.73	15.72	18.53	16.09
			Discarding ZZ and IC		
ED4	T_a	98.22	42.05	16.90	10.25
	T_c	40.73	30.29	15.12	10.24
ED3	T_a	98.15	42.04	16.90	10.25
	T_c	25.79	29.33	15.91	10.24
ED2	T_a	83.47	34.74	14.96	10.23
	T_c	6.22	14.92	12.83	10.21
ED1	T_a	42.71	30.42	19.45	16.09
	T_c	3.18	13.06	16.68	16.07
FSDT	T_a	43.97	30.37	19.30	16.09
	T_c	3.27	13.04	16.55	16.07
CLT	T_a	16.05	16.05	16.05	16.05
	T_c	1.196	6.895	13.77	16.03

Fourier Analyses of Various Temperature Distributions

Navier-type solutions can be extended to other types of applied loading unless an appropriate Fourier expansion is made for it. The benchmarks described in the next sections are related to various in-plane distributions of temperature. The appropriate Fourier expansion to these two cases should be written as

$$T_\Omega(x,y) = \sum_{m,n}^{R,Q} T_\Omega^{mn} \sin\frac{m\pi x}{a} \sin\frac{n\pi y}{b} \tag{40}$$

where R and Q are the maximum values of the considered m and n, while T_Ω^{mn} are the coefficients of the Fourier series.

NUMERICAL RESULTS

Most of the presented analyses refer to a thermomechanical problem for which the 3D exact solution has recently been provided by Bhaskar, Varadan, and Ali [4].

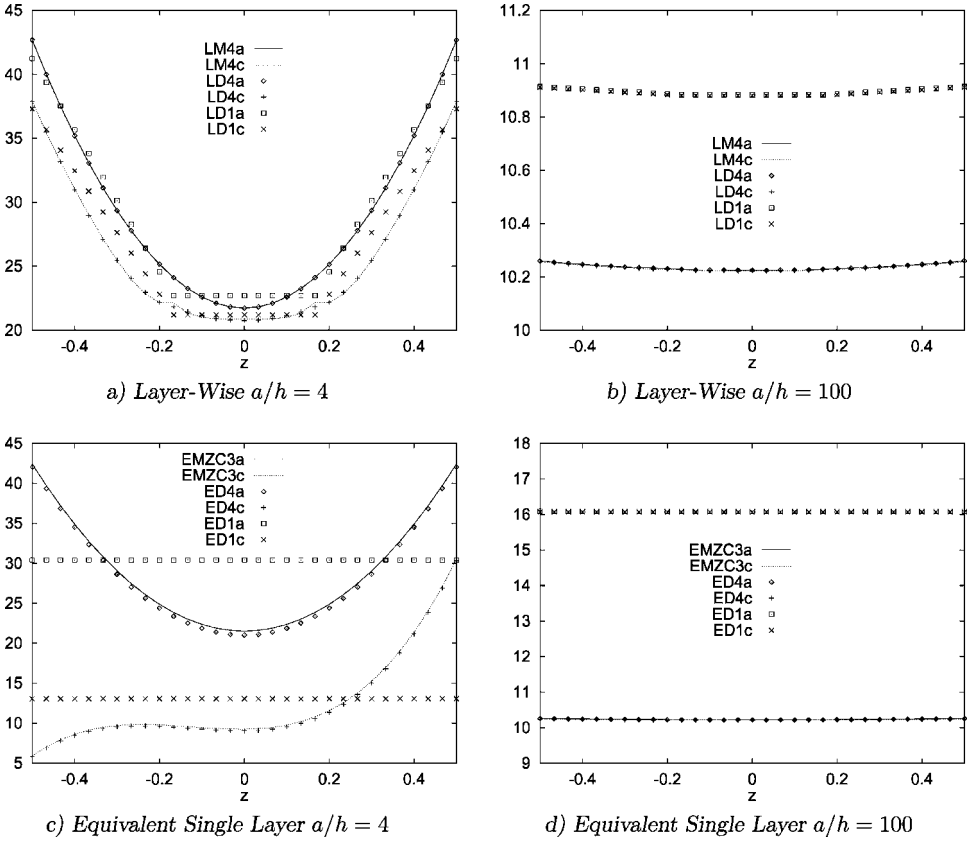

Figure 11. Transverse displacement $\bar{U}_z(a/2, b/2)$ distribution vs. z; comparison of various theories in the two cases of assigned and calculated temperature profiles.

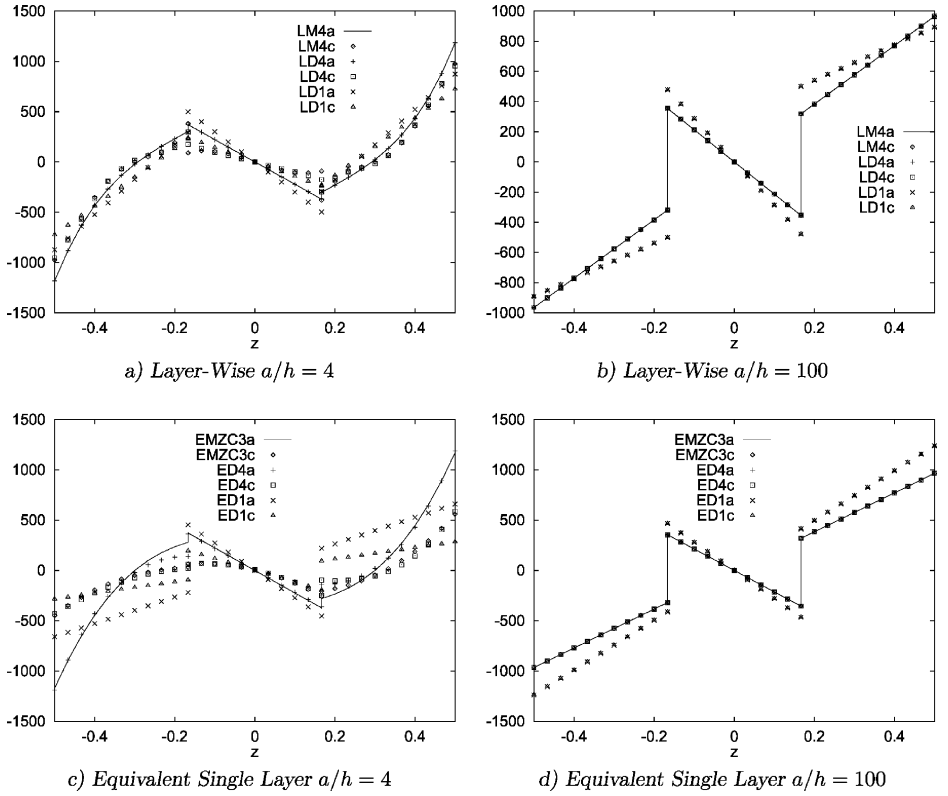

Figure 12. In plane normal stress $\bar{S}_{zz}(a/2, b/2)$ distribution vs. z; comparison of various theories in the two cases of assigned and calculated temperature profiles.

Numerical results are presented for a square plate loaded by various temperature fields. These fields are conveniently split as

$$T = T_P(z)T_\Omega(x, y)$$

As far as the temperature profile $T_P(z)$ is concerned, the assumed and calculated cases discussed in the second section have been considered. Concerning the in-plane $T_\Omega(x, y)$ distribution, the following cases have been treated (see Fig. 10):

- bi-sinusoidal distribution

$$T_\Omega = \sin\frac{\pi x}{a}\sin\frac{\pi y}{b}$$

- constant distribution

$$T_\Omega = 1 \tag{41}$$

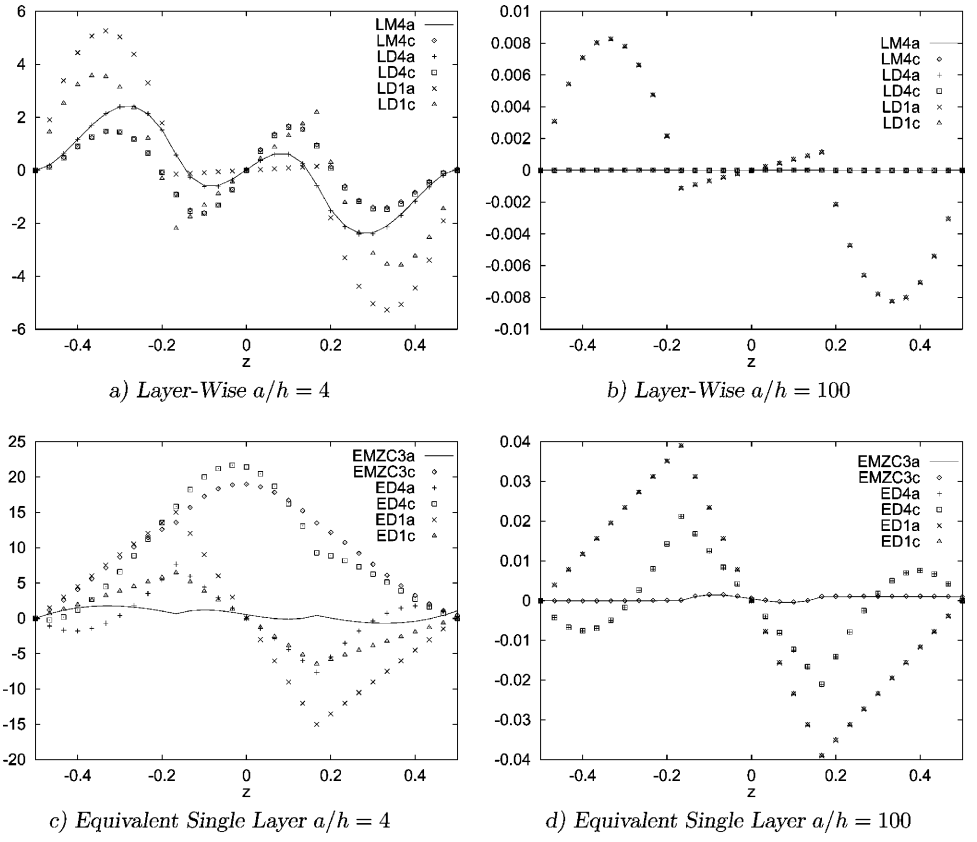

Figure 13. Out-of-plane normal stress $\bar{S}_{zz}(a/2, b/2)$ distribution vs. z; comparison of various theories in the two cases of assigned and calculated temperature profiles.

- triangular distribution

$$T_\Omega = \frac{x}{a} \tag{42}$$

- bitriangular (tentlike) distribution

$$\begin{aligned} T_\Omega &= \frac{2x}{a} \qquad 0 \le x \le \frac{a}{2} \\ T_\Omega &= \left(2 - \frac{2x}{a}\right) \qquad \frac{a}{2} < x \le a \end{aligned} \tag{43}$$

- localized distribution; the temperature heating is, in this case, applied to a small zone located in the plate center. This zone is a square area S^*,

$$S^* = \left[\frac{a}{10} * \frac{b}{10}\right]$$

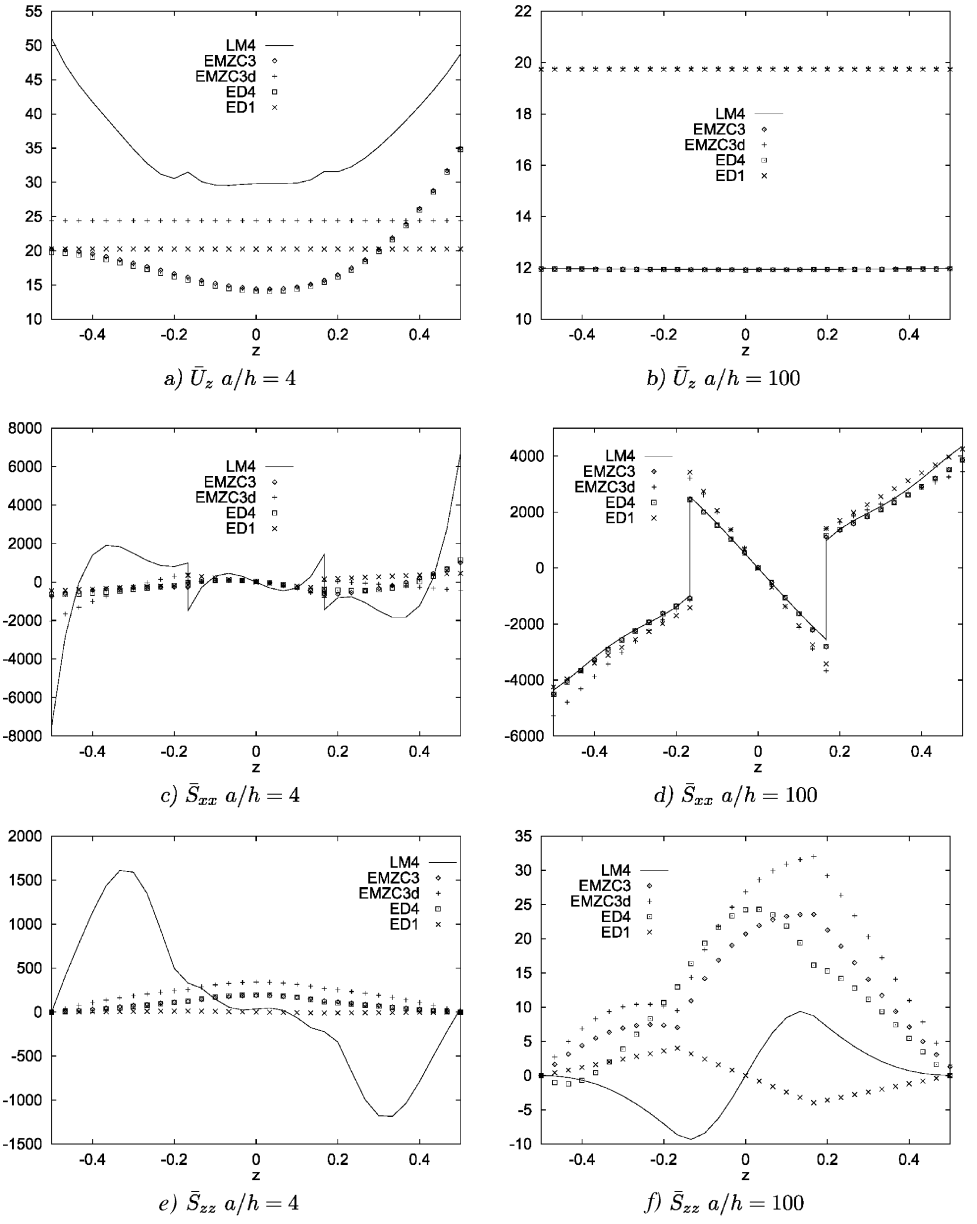

Figure 14. Stresses and displacements vs. z; comparison of significant theories in the case of in-plane uniform distribution of temperature.

Table 4 Influence of thickness ratio on stresses and displacements. Comparison among seven significant theories in the case of uniform temperature distribution and calculated temperature profile

a/h	2	4	10	100
		$U_z(a/2, b/2, h/2)$		
LM4	93.94	48.74	21.04	11.98
EMZC3	59.38	34.96	19.64	11.97
EDZ3	59.34	34.91	19.66	11.97
ED4	59.02	34.80	19.00	11.96
ED1	5.13	20.26	22.68	19.74
FSDT	5.13	20.26	22.68	19.74
CLT	1.91	10.32	18.06	19.68
		$S_{xx}(a/2, b/2, h/2)$		
LM4	0.5509E+4	0.6681E+4	0.6151E+4	0.4359E+4
EMZC3	0.5196E+3	0.1004E+4	0.1617E+4	0.3856E+4
EDZ3	0.5181E+3	0.1001E+4	0.1611E+4	0.3853E+4
ED4	0.7620E+3	0.1147E+4	0.1695E+4	0.3865E+4
ED1	0.1922E+3	0.4570E+3	0.1793E+4	0.4250E+4
FSDT	0.1922E+3	0.4570E+3	0.1793E+4	0.4250E+4
CLT	0.1521E+3	0.9446E+3	0.2331E+4	0.4484E+4
		$S_{zz}(a/2, b/2, h/6)$		
LM4	−0.2771E+3	−0.2229E+3	0.7871E+1	0.8724E+1
EMZC3	0.2702E+2	0.1272E+3	0.2609E+3	0.2356E+2
EDZ3	0.2636E+2	0.1253E+3	0.2751E+3	0.2193E+2
ED4	0.2344E+2	0.1139E+3	0.2379E+3	0.1613E+2
ED1	−0.3391E+1	−0.1125E+2	−0.9604E+1	−0.3991E+1
FSDT	−0.3391E+1	−0.1125E+2	−0.9604E+1	−0.3991E+1
CLT	0.9694E+1	0.1514E+3	0.6776E+3	0.2531E+4

in which case the temperature is considered to be constant:

$$T_\Omega = 1 \tag{44}$$

The thermomechanical properties of the lamina are

$$E_L/E_T = 25 \qquad G_{LT}/E_T = 0.5 \qquad G_{TT}/E_T = 0.2 \qquad \nu_{LT} = \nu_{TT} = 0.25$$
$$\alpha_T/\alpha_L = 1125 \qquad K_L = 36.42\,[\mathrm{W/m^oC^{-1}}] \qquad K_T = 0.96\,[\mathrm{W/m^oC^{-1}}]$$

where L and T refer to directions parallel and perpendicular, respectively, to the fibers (see [11] for notations).

A crossply, symmetrically laminated case $0^\circ/90^\circ/0^\circ$ was considered for all the treated problems. Unless otherwise stated, the deflection and stresses are presented in terms of the following dimensionless parameters:

$$\bar{U}_z = hu_z/(\alpha_L T_0 a^2) \qquad \bar{S}_{ij} = \sigma_{ij}/(E_T \alpha_L T_0)$$

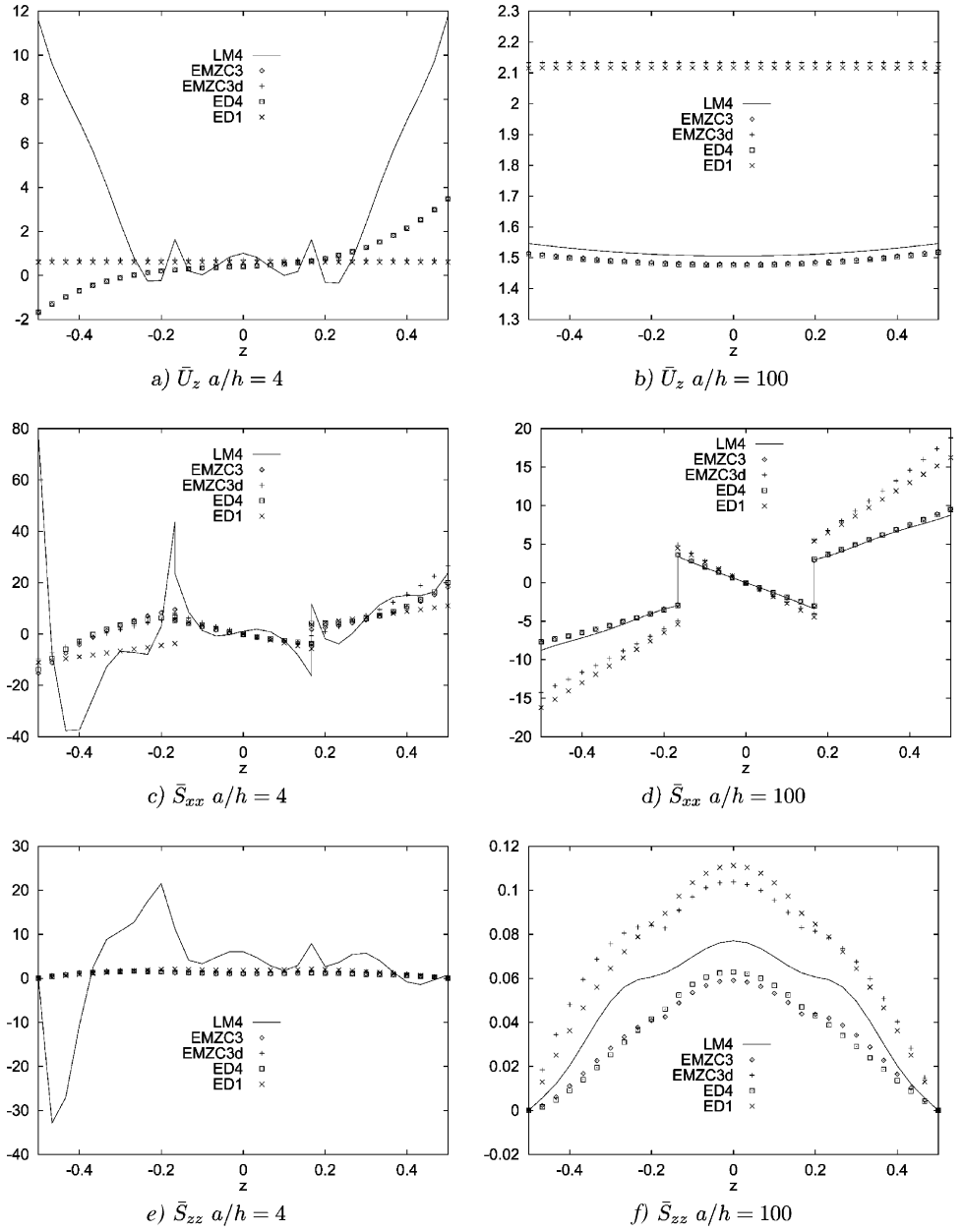

Figure 15. Stresses and displacements vs. z; comparison of significant theories in the case of in-plane localized distribution of temperature.

Table 5 Influence of thickness ratio on stresses and displacements. Comparison among seven significant theories in the case of triangular temperature distribution and calculated temperature profile

a/h	2	4	10	100
		$U\ (a/2,\ b/2,\ h/2)$		
LM4	46.97	24.37	10.52	5.99
EMZC3	29.69	17.48	9.82	5.98
EDZ3	29.67	17.45	9.83	5.98
ED4	29.51	17.40	9.50	5.98
ED1	2.57	10.13	11.34	9.87
FSDT	2.57	10.13	11.34	9.87
CLT	0.957	5.16	9.03	9.84
		$S_{xx}\ (a/2,b/2,h/2)$		
LM4	0.4344E + 3	0.6825E + 3	0.8108E + 3	0.8042E + 3
EMZC3	0.2498E + 3	0.3615E + 3	0.4473E + 3	0.7356E + 3
EDZ3	0.2490E + 3	0.3603E + 3	0.4459E + 3	0.7553E + 3
ED4	0.3579E + 3	0.3730E + 3	0.4269E + 3	0.7350E + 3
ED1	0.9634E + 1	0.2204E + 3	0.7356E + 3	0.8051E + 3
FSDT	0.9634E + 1	0.2204E + 3	0.7356E + 3	0.8051E + 3
CLT	0.7535E + 2	0.4409E + 3	0.8552E + 3	0.8071E + 3
		$S_{xz}\ (a/2,b/2,h/6)$		
LM4	0.5514E + 2	0.3177E + 2	0.5017E + 2	0.6903E + 1
EMZC3	0.1025E + 2	0.3667E + 2	0.4686E + 2	0.6676E + 1
EDZ3	0.1017E + 2	0.3653E + 2	0.4676E + 2	0.6669E + 1
ED4	0.6527E + 1	0.3674E + 2	0.4706E + 2	0.6631E + 1
ED1	0.8420E + 1	0.4825E + 2	0.5595E + 2	0.7740E + 1
FSDT	0.8420E + 1	0.4825E + 2	0.5595E + 2	0.7740E + 1
CLT	0.2792E + 2	0.8054E + 2	0.6101E + 2	0.7864E + 1

Comparison of Various Theories to Exact 3D Solutions

Table 1 compares the various theories to the 3D elasticity solution by Bhaskar et al. [4]. Transverse displacements and transverse shear stresses of thick and thin plates are compared in [4]. As in [4], the temperature is assumed to linearly vary through the plate thickness. The results of 25 theories are supplied. The comparisons in [12] have been extended. Very different accuracies can be obtained using different plate theories. Here, 23 theories were compared, including CLT (which is usually supposed to furnish the poorest description) and LM4 (which is supposed to give a quasi-3D description of stresses and displacements in laminated structures). Table 1 can therefore be used as a reference to assess any available theories as well as any future refinements of existing theories. The following main comments can be made.

1. With some exceptions for thin plates, the various theories predict similar results.
2. Higher order expansions (e.g., N values) are requested to capture the stress and displacement fields of thick plates.

Table 6 Influence of thickness ratio on stresses and displacements. Comparison among seven significant theories in the case of bitriangular temperature distribution and calculated temperature profile

a/h	2	4	10	100
		$U\ (a/2,\ b/2,\ h/2)$		
LM4	69.56	34.59	14.23	7.74
EMZC3	37.83	22.58	12.94	7.73
EDZ3	37.81	22.55	12.94	7.73
ED4	37.61	22.49	12.54	7.73
ED1	3.27	12.93	14.56	12.81
FSDT	3.27	12.93	14.56	12.81
CLT	1.22	6.58	11.61	12.77
		$S_{xx}(a/2,\ b/2,\ h/2)$		
LM4	0.9586E + 3	0.1027E + 4	0.1192E + 4	0.1308E + 4
EMZC3	0.3303E + 3	0.5884E + 3	0.6809E + 3	0.1198E + 4
EDZ3	0.3293E + 3	0.5863E + 3	0.6786E + 3	0.1198E + 4
ED4	0.4836E + 3	0.6225E + 3	0.6487E + 3	0.1197E + 4
ED1	0.1224E + 2	0.2902E + 3	0.1074E + 4	0.1332E + 4
FSDT	0.1224E + 2	0.2902E + 3	0.1074E + 4	0.1332E + 4
CLT	0.9684E + 2	0.5962E + 3	0.1314E + 4	0.1336E + 4
		$S_{zz}(a/2,\ b/2,\ h/6)$		
LM4	− 0.370E + 2	0.5596E + 1	0.4203E + 2	0.3377E + 1
EMZC3	0.1733E + 2	0.8254E + 2	0.7613E + 2	0.7534E + 1
EDZ3	0.1691E + 2	0.8138E + 2	0.1345E + 3	0.7005E + 1
ED4	0.1504E + 2	0.7403E + 2	0.1245E + 3	0.5477E + 1
ED1	− 0.2157E + 1	− 0.6937E + 1	− 0.3616E + 1	− 0.4153E − 1
FSDT	− 0.2157E + 1	− 0.6937E + 1	− 0.3616E + 1	− 0.4153E − 1
CLT	0.6178E + 1	0.9627E + 2	0.4003E + 3	0.1074E + 4

3. The description of the ZZ effect leads to significant improvements in both PVD and RMVT applications. The MZZF remarkably improves the related results: the EDZ analyses are more accurate than the ED ones.
4. CLT and FSDT analyses can lead to large error in predicting the thermal response of laminate plates.
5. The fulfillment of IC leads to improvements in RMVT formulated theories.
6. LWM descriptions are more accurate than the corresponding ESLM ones. On the other hand, LWMs are more computationally expensive than ESLMs.
7. Mixed descriptions, based on RMVT, are more accurate than the corresponding formulation based on PVD. This implies that the a priori fulfillment of IC leads to improved displacements and stresses.
8. RMVT is much more effective for ESLM formulations.
9. Different degrees of accuracy have been found for displacement evaluations compared to transverse shear stress ones.
10. The difficulties that theories with linear displacement fields in z exhibit should be noted when considering a linear temperature profile. That happens for both thin and thick plates [12].

Table 7 Influence of thickness ratio on stresses and displacements. Comparison among seven significant theories in the case of localized temperature distribution and calculated temperature profile

a/h	2	4	10	100
		$\bar{U}(a/2, b/2, h/2)$		
LM4	27.18	11.77	4.210	1.546
EMZC3	21.57	3.489	3.215	1.522
EDZ3	2.156	3.488	3.213	1.522
ED4	2.169	3.482	3.189	1.518
ED1	1.284	5.942	1.232	2.116
FSDT	1.284	5.942	1.232	2.116
CLT	0.0494	0.3438	1.061	2.097
		$\bar{S}_{xx}(a/2, b/2, h/2)$		
LM4	0.4027E + 2	0.2372E + 2	0.1896E + 2	0.8769E + 1
EMZC3	0.1112E + 2	0.1822E + 2	0.2188E + 2	0.9544E + 1
EDZ3	0.1107E + 2	0.1818E + 2	0.2194E + 2	0.9547E + 1
ED4	0.1348E + 2	0.2003E + 2	0.2113E + 2	0.9505E + 1
ED1	0.5168E + 0	0.1104E + 2	0.2409E + 2	0.1623E + 2
FSDT	0.5168E + 0	0.1104E + 2	0.2409E + 2	0.1623E + 2
CLT	0.3512E + 1	0.1615E + 2	0.1932E + 2	0.1602E + 2
		$\bar{S}_{zz}(a/2, b/2, h/6)$		
LM4	−0.7655E + 1	0.7882E + 1	0.1432E + 1	0.6245E − 1
EMZC3	0.1855E + 0	0.1148E + 1	0.1131E + 1	0.4387E − 1
EDZ3	0.1809E + 0	0.1146E + 1	0.1136E + 1	0.4393E − 1
ED4	0.2003E + 0	0.1231E + 1	0.1153E + 1	0.4699E − 1
ED1	0.4093E + 0	0.2103E + 1	0.1646E + 1	0.8952E − 1
FSDT	0.4093E + 0	0.2103E + 1	0.1646E + 1	0.8952E − 1
CLT	0.1278E + 1	0.2687E + 1	0.1193E + 1	0.1004E + 0

11. EDZ3 consists of the best ESLM multilayered theories in the framework of classical theories with only displacement unknowns and PVD applications.
12. EMZC3 consists of the best ESLM multilayered theories.
13. LM4 gives a quasi-3D description of displacement and stress fields of thermally loaded plates.

Influence of the Temperature Profile: Comparison with Assumed Linear and Calculated Cases

An exaustive comparison of different theories considering assumed linear and calculated temperature profiles is given in Tables 2 and 3 and Figure 11, 12, and 13. The problem was discussed in a more complete form in the literature [18]. Very thick ($a/h = 2$), thick ($a/h = 4$), moderately thick ($a/h = 10$), and thin plates ($a/h = 100$) were considered. A 3D solution for the calculated temperature profiles is not available. However, according to analyses in Table 1, LM4 results should be taken as a quasi-3D description in the case of calculated temperature profiles. In addition to the comments of the previous section, the following should be noticed.

1. The error introduced by the different theories is now also due to their capacity to capture the $T(z)$ profiles as they come from Eq. (5).
2. The differences between T_a (assumed linear $T_P(z)$) and T_c (calculated $T_P(z)$) are very significant. In particular, such differences

   - are very significant for both RMVT and PVD plate theories.
   - are larger for ESLMs than LWMs.
   - increase very much for low values of N.
   - increase as the thickness parameter decreases.

3. The 3D elasticity solutions that refer to linear $T_P(z)$ can be ineffective even though moderately thick plates are considered.
4. The previously underlined differences should be related to the layerwise form of T_c, as discussed in the second section. Such a layerwise form is difficult to capture using ESLMs or lower order LWMs.
5. The plots given in Figures 11, 12, and 13 show that the differences among the several theories depend on the position of z. In particular, the main discrepancies among the different theories occur in conjunction to the layer interfaces.

It can be concluded that an accurate thermal stress analysis can be meaningless unless the calculated temperature profile is considered in the calculations.

Comparison of the Prediction of Significant Theories Based on Various In-Plane Distributions of Applied Temperature

This paragraph considers those thermal loading problems that have been treated by means of Fourier series. According to the conclusion reached in the previous paragraph, the numerical results were restricted to calculate temperature profiles. Furthermore, for the sake of brevity, only a few significant theories are compared. Among the significant theories, the following have been considered:

LM4, which represents the quasi-3D solutions;
EMZC3, which represents the most accurate ESLM description;
EDZ3, which includes a ZZ term in classical higher order theories with only displacement;
ED4, which is the best classical higher order model;
ED1, which is the refinement of an FSDT and includes transverse normal strain effects; and
FSDT and CLT.

The Taylor series was arrested at the values $M = N = 25$ (that is, 625 terms were used), which have shown convergent solutions for all the considered problems. The results quoted in this paragraph could be used to assess approximated solution techniques such as finite element methods.

Uniform distribution. Transverse displacement, in-plane normal, and transverse normal stresses are compared in Table 4. Values are given for various thickness

parameters. Due to the fact that the temperature profile coincides with the calculated ones (see second section), the difference in the predictions among the considered theories increases with respect to the ones in Table 1. The through-the-thickness distributions are plotted in Figure 14 for thick- and thin-plate geometries.

Triangular distribution. The results are shown in Table 5. Such a loading case can be very common in many practical problems. The same comments that were made for the previous case are also valid here.

Bitriangular distribution. This is a so-called tentlike problem [10]. Such a temperature distribution can be generated, for example, if the plate is heated by a hot tube crossing the plate center and parallel to the two edges. The results are given in Table 6. The same comments that were made for the previous case are also valid here.

Localized distribution. This case considers the localized heating of the plate. The results are given in Table 7 and Figure 15. The variations in the stress fields in the three layers are higher than the previous cases.

CONCLUDING REMARKS

This paper has compared classical and advanced theories for the analysis of the thermomechanical response of multilayered plates. Various temperature distributions have been considered in both the thickness and in-plane directions. The following main conclusions can be made.

1. An accurate description of the stress and displacement fields can be meaningless unless an accurate description is made of the temperature profile in the thickness direction.
2. Refined theories could be required for an accurate description of the stress and displacement field of both thick- and thin-plate geometries.
3. The results supplied in this paper can be used to validate approximate solution procedures, such as the finite element method.

REFERENCES

1. S. Srinivas and A. K. Rao, A Note on Flexure of Thick Rectangular Plates and Laminates with Variation of Temperature Across the Thickness, *B. Acad. Pol. Sci. Tech.*, vol. 20, pp. 229–234, 1972.
2. M. N. Bapu Rao, 3D Analysis of Thermally Loaded Thick Plates, *Nucl. Eng. Des.*, vol. 55, pp. 353–361, 1979.
3. V. B. Tungikar and K. M. Rao, Three Dimensional Exact Solution of Thermal Stresses in Rectangular Composite Laminates, *Compos. Struct.*, vol. 27, pp. 419–427, 1994.
4. K. Bhaskar, T. K. Varadan, and J. S. M. Ali, Thermoelastic Solution for Orthotropic and Anisotropic Composites Laminates, *Compos., B.*, vol. 27B, pp. 415–420, 1996.
5. E. Carrera, A Class of Two-Dimensional Theories for Anisotropic Multilayered Plates Analysis, *Acad. Sci. Torino*, vol. 19–20, pp. 1–39, 1995.

6. T. R. Tauchert, Thermally Induced Flexure, Buckling and Vibration of Plates, *Appl. Mech. Rev.* vol. 44, pp. 347–360, 1991.
7. A. K. Noor and W. S. Burton, Computational Models for High-Temperature Multilayered Composite Plates and Shells, *Appl. Mech. Rev.*, vol. 45, pp. 419–446, 1992.
8. J. Argyris and L. Tenek, Recent Advances in Computational Thermo-Structural Analysis of Composite Plates and Shells with Strong Nonlinearities, *Appl. Mech. Rev.*, vol. 50, pp. 285–306, 1998.
9. L. Librescu, *Elasto-statics and Kinetics of Anisotropic and Heterogeneous Shell-Type Structures*, Noordhoff Int., Leyden, The Netherlands, 1975.
10. E. A. Thornton, *Thermal Structures for Aerospace Applications*, Educational Series, American Institute of Aeronautics and Astronautics, Reston, VA, 1996.
11. J. N. Reddy, *Mechanics of Laminated Composite Plates, Theory and Analysis*, CRC Press, Boca Raton, 1997.
12. E. Carrera, An Assessment of Mixed and Classical Theories for the Thermal Stress Analysis of Orthotropic Plate Multilayerd Plates, *J. Thermal Stresses*, vol. 23, pp. 797–831, 2000.
13. K. N. Cho, C. W. Bert, and A. G. Striz, Thermal Stress Analysis of Laminate Using Higher Order Individual-Layer Theory, *J. Thermal Stresses*, vol. 12, pp. 321–332, 1989.
14. H. Murakami, Assessment of Plate Theories for Treating the Thermo-Mechanical Response of Layered Plates, *Compos. Eng.*, vol. 3, pp. 137–149, 1993.
15. J. S. M., Ali, K. Bhaskar, and T. K. Varadan, A New Theory for Accurate Thermal/Mechanical Flexural Analysis of Symmetric Laminated Plates, *Compos. Struct.*, vol. 45, pp. 227–232, 1996.
16. X. Zhou, A. Chattopadhyay, and H. Gu, Dynamic Response of Smart Composites Using a Coupled Thermo-Piezoelectric-Mechanical Model, *AIAA J.*, vol. 38, pp. 1939–1948, 2000.
17. H. Gu, A. Chattopadhyay, J. Li, and X. Zhou, Higher Order Temperature Theory for Coupled Thermo-Piezoelectric-Mechanical Modeling of Smart Composites, *Int. J. Solid Struct.*, vol. 37, pp. 6479–6497, 2000.
18. E. Carrera, Temperature Profile Influence on Layered Plates Response Considering Classical and Advanced Theories, *AIAA J.*, vol. 9, pp. 1885–1896, 2002.
19. H. Murakami, Laminated Composite Plate Theory with Improved In-Plane Response, *J. Appl. Mech.*, vol. 53, pp. 661–666, 1986.
20. E. Reissner, On a Certain Mixed Variational Theory and a Proposed Application, *Int. J. Numer. Method Eng.*, vol. 20, pp. 1366–1368, 1984.
21. E. Carrera, Developments, Ideas and Evaluations Based upon the Reissner's Mixed Variational Theorem in the Modeling of Multilayered Plates and Shells, *App. Mech. Rev.*, vol. 54, pp. 301–329, 2001.
22. E. Carrera, Evaluation of Layer-Wise Mixed Theories for Laminated Plates Analysis, *AIAA, J.*, vol. 36, pp. 830–839, 1998.
23. E. Carrera, A Study of Transverse Normal Stress Effects on Vibration of Multilayered Plates and Shells, *J. Sound Vib.*, vol. 225, pp. 803–829, 1999.
24. E. Carrera, and L. Demasi, Two Benchmark Studies of Transverse Normal Stress Effects on Vibration of Multilayered Plates and Shells, *AIAA, J.*, vol. 41, pp. 1356–1562, 2003.